High-resolution analytical electron microscopy of catalytically etched silicon nanowires

M. Schade · N. Geyer · B. Fuhrmann · F. Heyroth · H.S. Leipner

Abstract We report on the characterization of hexagonally ordered, vertically aligned silicon nanowires (SiNW) by means of analytical transmission electron microscopy. Combining colloidal lithography, plasma etching, and catalytic wet etching arrays of SiNW of a sub-50 nm diameter with an aspect ratio of up to 10 could be fabricated. Scanning transmission electron microscopy has been applied in order to investigate the morphology, the internal structure, and the composition of the catalytically etched SiNW. The analysis yielded a single-crystalline porous structure composed of crystalline silicon, amorphous silicon, and SiO_x with $x \leq 2$.

PACS 61.46.Km · 68.37.Ma · 82.45.Vp

1 Introduction

Silicon nanowires (SiNW) are potential candidates for applications in electronics, photonics, and thermoelectrics. Compared with bulk silicon, a change in characteristic properties is expected due to the size. Therefore, the possibility to control these features by varying the size, the morphology, or the surface structure is indispensable. On the basis of the well-known vapor–liquid–solid process [1], fabrication methods like chemical vapor deposition, molecular beam epitaxy, and solution growth have been developed in order to grow SiNW following the "bottom-up" approach. In addition, also "top-down" approaches have been developed successfully in order to improve the regularity of the SiNW [2]. The combination of colloidal lithography, plasma etching, and chemical wet etching produces SiNW with well-defined length, diameter, density, and arrangement.

The fabrication principle is based on a metal-induced local oxidation and dissolution of silicon in a solution containing fluorine ions, where the metal acts as a catalyst [3, 4]. In this galvanic exchange process the metal (e.g., Ag, Au, or Pt) layer represents a local cathode and the silicon substrate serves as an anode. The etching solution consists of H_2O_2 and HF. H_2O_2 oxidizes the silicon substrate under the generation of SiF_4, which is removed by HF subsequently. This process can be specified by the chemical reactions given by Li et al. [5]. The oxidation process generates pits in the silicon substrate where the metal layer sinks in so that a stable reaction is formed. The areas that are not covered with the metal stay non-etched.

2 Experimental details

Mirror-polished arsenic-doped n-type Si(111)-wafers with a resistivity between 0.001 and 0.006 Ωcm have been used. The substrate was cut into 10 mm × 10 mm pieces, which were treated afterwards for 15 min at 348 K in an RCA solution, containing H_2O_2 (30 wt.%), NH_4OH (25 wt.%), and H_2O at a volume ratio of 1:1:5, in order to remove organics. Subsequently, the substrate was immersed in deionized water. Close-packed monolayers of monodisperse polystyrene spheres with diameters of 200 nm, received from microparticles GmbH (Germany) as a 10 wt.% water solution, were deposited on the cleaned silicon substrate via colloidal lithography. Oxygen plasma at a flow rate of 400 sccm/min and a pressure of 0.06 mbar was applied in order to reduce the

M. Schade (✉) · N. Geyer · B. Fuhrmann · F. Heyroth · H.S. Leipner
Interdisziplinäres Zentrum für Materialwissenschaften, Martin-Luther-Universität Halle-Wittenberg, 06099 Halle, Germany
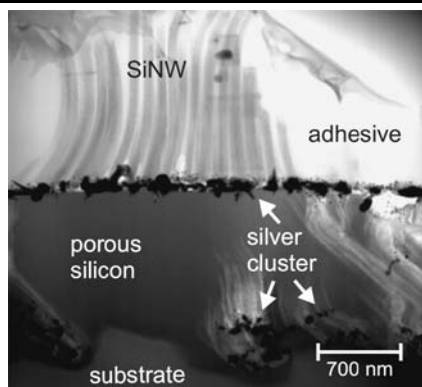e-mail: martin.schade@cmat.uni-halle.de
Fax: +49-345-5527390

Fig. 1 Bright-field STEM image of a cross-section sample

Fig. 2 Diffraction patterns of **a** the porous layer or the substrate, respectively, and **b** one SiNW

Fig. 3 Silicon $L_{2,3}$ edges of bulk silicon, amorphous silicon, SiO_2, and a SiNW and the corresponding MLS fit

diameter of the spheres as well as transforming the close-packed monolayer masks into a non-close-packed assembly. These modified masks were covered with a 15 nm thick silver layer by thermal evaporation (HVT B 30.2 system). The polystyrene spheres were removed subsequently in an ultrasonic bath consisting of $CHCl_3$. Finally, the silicon wafer covered with the silver mask was immersed in an etching mixture consisting of HF and H_2O_2 with concentrations of 4.6 or 0.44 M, respectively, (at room temperature) so that SiNW were formed.

In order to investigate the internal structure and the composition of the nanowires, electron-transparent cross-section samples have been prepared by applying the standard preparation of mechanical grinding, polishing, dimpling, and Ar ion milling. The samples have been investigated by analytical transmission electron microscopy using a VG HB 501 UX scanning transmission electron microscope (STEM) equipped with a Gatan ENFINA 1000 parallel electron energy-loss spectrometer and an EUMEX energy dispersive X-ray detector. The acceleration voltage was 100 kV.

3 Results and discussion

An overview of a typical sample is given in Fig. 1. Some SiNW are curved or broken as a result of the cross-section preparation. A porous silicon layer and the crystalline silicon substrate are visible beneath the SiNW. They can be distinguished through the change in the contrast at their border. The SiNW are separated from the porous layer by a chain of silver clusters. However, there are also bigger silver clusters beneath this chain deep in the porous layer. The silver has been identified by energy-dispersive X-ray spectroscopy. At sample position where bigger silver particles break through the silver chain no SiNW are existent. Though, it has to be noticed that a possible influence of the sample preparation on such a behavior could not be excluded.

It is well-known that porous silicon may be formed by catalytic etching through the generation of pits in crystalline
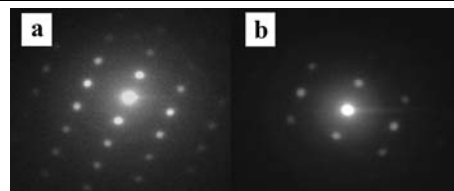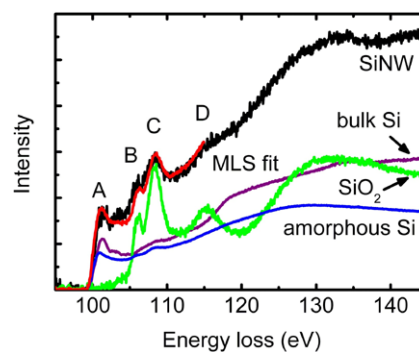
silicon [6]. This process does not imply a loss in crystallinity. In order to verify this assumption, electron diffraction patterns of one single SiNW on the one hand and of both the porous layer and the silicon substrate on the other hand were recorded. Due to the fact that the diffraction pattern of the substrate and the porous layer were identical, only one of them is shown in Fig. 2a. The lower thickness of the SiNW causes the visibility of only a few diffraction spots in Fig. 2b. Nevertheless, both patterns in Fig. 2 represent the same crystalline structure. We conclude that the SiNW as well as the porous layer consist of a single-crystalline skeleton, which is filled by silicon oxide.

Electron energy-loss (EEL) spectroscopy has been applied in order to receive further information about both the structure and the composition of the SiNW. EEL spectra of the silicon $L_{2,3}$ edges from a SiNW as well as from a bulk silicon, from reference amorphous silicon and from reference SiO_2, have been recorded with a measuring time of 3 s per spectrum. The $L_{2,3}$ edges are shown in Fig. 3 after a background correction with a power law. Referring to Li et al. [5], the SiNW consists only of SiO_2 and bulk silicon or amorphous silicon, respectively. Hence, we assumed the silicon $L_{2,3}$ edges of the SiNW to be a superposition of the silicon $L_{2,3}$ edges of bulk silicon, amorphous silicon, and SiO_2. Its structure exhibits four main features (labeled A to D in Fig. 3) that could be well-assigned: Peak A is characteristic for bulk silicon or amorphous silicon, respectively, while the peaks B to D arise from the presence of SiO_2. In order to quantify the ratio of the constituents mentioned in
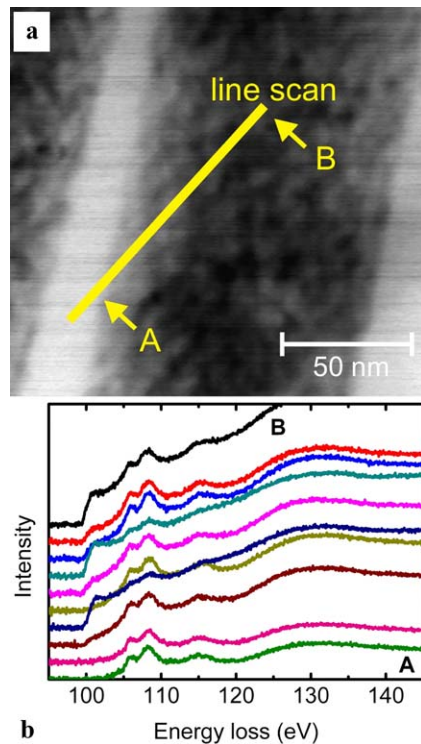
Fig. 4 **a** BF STEM image of a SiNW with a linescan indicated. **b** EEL spectra between the marks A and B. The particular spectra are shifted in the intensity for a better visibility

SiNW, a multiple least squares procedures (MLS) was applied [7]. The spectra of bulk silicon, amorphous silicon, and SiO_2 in Fig. 3 were used as a reference for the MLS procedure. The MLS fit is also illustrated in Fig. 3: The fit worked very well at the peaks A and C but, for instance, between the peaks A and B it failed. The more detailed investigation of the composition reveals that other constituents of silicon oxide (SiO_x with $x \leq 2$) have to appear inside the SiNW. This conclusion is supported by the measurement of spectra where instead of peak A only a shoulder at peak B has occurred. These spectra could not be fitted sufficiently with the reference spectra used.

Figure 4a shows the bright-field (BF) image of a SiNW where the porous surface structure is clearly visible. In order to obtain spectra from the surface region as well as from the interior a line scan across the SiNW has been carried out with an average measuring time of 2.5 s per measuring point. The silicon $L_{2,3}$ edges, obtained after background correction, are given in Fig. 4b. The two lower spectra measured

next to position A (surface region of the SiNW) are comparable to the spectrum of SiO_2 in Fig. 3. This fact indicates that the SiNW are surrounded by a thin SiO_2 layer. The other spectra in Fig. 4b can be interpreted again as a superposition of the silicon $L_{2,3}$ edges of bulk silicon, amorphous silicon, and SiO_x ($x \leq 2$). The alternating shape of the silicon $L_{2,3}$ edges along the line scan reflects the inhomogeneity inside the SiNW that is caused by the porous structure: Following the line scan from the surface region of the SiNW to its center the EEL spectra show no correlation between the position at the SiNW and its composition or structure, respectively.

We described the characterization of vertically aligned SiNW fabricated by catalytic etching. Both the internal structure and the composition of these catalytically etched SiNW were investigated by analytic electron microscopy. STEM images show the porous structure of the SiNW. An additional porous silicon layer is formed beneath the SiNW in the substrate. Diffraction patterns show that the SiNW as well as the porous layer consist of a single-crystalline skeleton filled by silicon oxide. The crystal structure of the skeleton is the same as the silicon substrate. The SiNW mainly consist of a mixture of bulk silicon and SiO_2, whereas no correlation between the varying composition and the position at the SiNW exists. Due to the differences between the recorded spectra and the corresponding MLS fits in the 101–105 eV energy-loss range, the presence of intermediate oxidation states of silicon oxide (i.e., Si^{3+}, Si^{2+}, Si^{1+}) is assumed [8]. A possible influence of quantum confinement effects on the EEL spectra due to the micropores has been neglected in this paper and has to be a subject of the further research.

References

1. R.S. Wagner, W.C. Ellis, Appl. Phys. Lett. **4**, 89 (1964)
2. B. Fuhrmann, H.S. Leipner, H.-R. Höche, L. Schubert, U. Gösele, Nano. Lett. **5**, 2524 (2005)
3. Z. Huang, H. Fang, J. Zhu, Adv. Mater. **19**, 744 (2007)
4. K. Peng, J. Hu, Y. Yan, Y. Wu, H. Fang, Y. Xu, S.T. Lees, J. Zhu, Adv. Funct. Mater. **16**, 387 (2006)
5. X. Li, W. Bohn, Appl. Phys. Lett. **77**, 2572 (2000)
6. H. Föll, M. Christophersen, J. Carstensen, G. Hasse, Mater. Sci. Eng. R **39**, 93 (1981)
7. R. Leapman, *Transmission Electron Energy Loss Spectroscopy in Materials Science and the EELS Atlas* (Wiley, Weinheim, 2004), pp. 70–75
8. L. Dori, J. Bruley, D.J. DiMaria, P.E. Batson, J. Tornello, M. Arienzo, J. Appl. Phys. **69**(4), 2317 (1991)